

The Role of Chloroplast Electron Transport and Metabolites in Modulating Rubisco Activity in Tobacco. Insights from Transgenic Plants with Reduced Amounts of Cytochrome *b/f* Complex or Glyceraldehyde 3-Phosphate Dehydrogenase¹

Sari A. Ruuska², T. John Andrews, Murray R. Badger, G. Dean Price, and Susanne von Caemmerer*

Molecular Plant Physiology (S.A.R., T.J.A., M.R.B., G.D.P., S.v.C.) and Photobioenergetics (S.A.R., S.v.C.) Groups, Research School of Biological Sciences, The Australian National University, G.P.O. Box 475, Canberra, Australian Capital Territory 2601, Australia

Leaf metabolites, adenylates, and Rubisco activation were studied in two transgenic tobacco (*Nicotiana tabacum* L. cv W38) types. Plants with reduced amounts of cytochrome *b/f* complex (anti-*b/f*) have impaired electron transport and a low transthylakoid pH gradient that restrict ATP and NADPH synthesis. Plants with reduced glyceraldehyde 3-phosphate dehydrogenase (anti-GAPDH) have a decreased capacity to use ATP and NADPH in carbon assimilation. The activation of the chloroplast NADP-malate dehydrogenase decreased in anti-*b/f* plants, indicating a low NADPH/NADP⁺ ratio. The whole-leaf ATP/ADP in anti-*b/f* plants was similar to wild type, while it increased in anti-GAPDH plants. In both plant types, the CO₂ assimilation rates decreased with decreasing ribulose 1,5-bisphosphate concentrations. In anti-*b/f* plants, CO₂ assimilation was further compromised by reduced carbamylation of Rubisco, whereas in anti-GAPDH plants the carbamylation remained high even at subsaturating ribulose 1,5-bisphosphate concentrations. We propose that the low carbamylation in anti-*b/f* plants is due to reduced activity of Rubisco activase. The results suggest that light modulation of activase is not directly mediated via the electron transport rate or stromal ATP/ADP, but some other manifestation of the balance between electron transport and the consumption of its products. Possibilities include the transthylakoid pH gradient and the reduction state of the acceptor side of photosystem I and/or the degree of reduction of the thioredoxin pathway.

Plants are subjected to fluctuating environmental conditions, which result in changes in the supply of light and CO₂ for photosynthesis. Regulatory mechanisms exist in the chloroplasts, which match the rates of electron transport with carbon assimilation to ensure the coordination of the photosynthetic reactions. The PCR and photorespiratory cycles consume ATP and NAD(P)H produced by chloroplast electron transport and the availability of these compounds affects their functioning. Several photosynthetic

enzymes are regulated by metabolites, either by their end products or intermediates occurring later in the PCR cycle (for review, see Stitt, 1996). Linear electron transport also leads to alkalization and an increase in the Mg²⁺ concentration in the stroma (Heldt, 1979; Portis, 1981). Many PCR cycle enzymes have a pH optimum around 8.0 and require Mg²⁺ as a cofactor, so these light-induced ionic movements promote their activation. In addition, many chloroplast enzymes are light regulated via the ferredoxin-thioredoxin pathway (Buchanan, 1984).

The activity of Rubisco also changes in vivo. The activation of Rubisco generally increases as light intensity increases (Mächler and Nösberger, 1980; von Caemmerer and Edmondson, 1986) and deactivation is sometimes observed when stromal inorganic phosphate is depleted (Sharkey, 1990). Rubisco is active only when a specific lysyl residue within its catalytic site is carbamylated (complexed with CO₂) and bound with Mg²⁺. This carbamylation process is considered to be enhanced by the light-dependent stromal alkalization and increase in Mg²⁺ concentration (Lorimer et al., 1976; Andrews and Lorimer, 1987). However, it is evident that, in vivo, the changes in carbamylation state are mediated by another stromal protein, Rubisco activase (Somerville et al., 1982; Salvucci et al., 1985).

Activase requires ATP hydrolysis to function and is inhibited by ADP, so presumably it is sensitive to the stromal ATP/ADP ratio (Robinson and Portis, 1988; Wang and Portis, 1992). This may not be the only mechanism regulating Rubisco activase. The transthylakoid proton gradient and electron transport may also be involved in mediating the response of its activity to light (Campbell and Ogren, 1990a, 1992). Additionally, the activity of Rubisco is affected by chloroplast metabolites. Phosphorylated compounds, including the substrate ribulose 1,5-bisphosphate (RuBP), can bind to uncarbamylated sites preventing activation (Portis, 1995). Rubisco activase facilitates the detachment of these compounds and thus promotes carbamylation and catalysis. The relationship between Rubisco and RuBP concentration is complicated because under some conditions, the carbamylation may be promoted by the presence of RuBP (Mate et al., 1996).

In this study we used two different transgenic tobacco (*Nicotiana tabacum*) types to investigate the interactions

¹ This work was supported in part by an Australian National University Doctoral Scholarship, an Overseas Postgraduate Research Scholarship, and a grant from the Academy of Finland to S.A.R.

² Present address: Department of Botany and Plant Pathology, Michigan State University, East Lansing, MI 48824.

* Corresponding author; e-mail susanne@rsbs.anu.edu.au; fax 61-2-6249-5075.

between chloroplast light reactions and carbon metabolism. Plants with reduced amounts of the chloroplast cytochrome (Cyt) *b/f* complex (anti-*b/f* plants) have a decreased electron transport capacity, which should lead to a low transthylakoid pH gradient (ΔpH) and a reduction in the ATP and NADPH synthesis (Price et al., 1995b, 1998). In contrast, plants with a reduction in the activity of glyceraldehyde 3-phosphate dehydrogenase (anti-GAPDH plants) have a decreased capacity to use ATP and NADPH in carbon assimilation and have a high ΔpH (Price et al., 1995a). We studied the energy status of these contrasting plant types by measuring the whole-leaf adenylate levels. In addition, we used the activation state of chloroplast NADP-dependent malate dehydrogenase (NADP-MDH) as an indicator of the stromal NADPH/NADP⁺ ratio. These measurements enabled us to evaluate how the electron transport rate, transthylakoid pH gradient, ATP/ADP ratio, and RuBP concentration interact in determining the degree of Rubisco activation and how the activity of Rubisco activase may be regulated in response to the light signal in chloroplasts.

MATERIALS AND METHODS

Plant Material and Growth Conditions

The transformation of tobacco (*Nicotiana tabacum* L. cv W38) with an antisense construct directed against the Rieske FeS subunit of the chloroplast Cyt *b/f* complex (FeS) (referred to as anti-*b/f* plants) has been described previously (Price et al., 1995b). Antisense plants in this study were raised from selfed T₃ seeds of the line B6F-2.2-513-16, producing a range of phenotypes in respect to FeS protein content and CO₂ assimilation rates (Price et al., 1998). Both untransformed W38 and antisense plants were grown in 5-L pots in a growth cabinet and fertilized with Hewitt's complete nutrient solution (Hewitt and Smith, 1975) three times a week. The light intensity was 100 to 120 $\mu\text{mol quanta m}^{-2} \text{s}^{-1}$, the photoperiod was 20 h, and the temperature was kept constant at 25°C. The low growth irradiance and long days were used to minimize the instability of the antisense phenotype (Price et al., 1995b). The anti-glyceraldehyde 3-phosphate dehydrogenase (anti-GAPDH) plants were grown from T₁ seeds of plant GAP-R (Price et al., 1995a), and had a variety of GAPDH activities. Anti-GAPDH and untransformed W38 tobacco plants were grown in an air-conditioned greenhouse where the peak photon flux density was 700 to 900 $\mu\text{mol m}^{-2} \text{s}^{-1}$. The plants were used at 8 to 16 weeks after germination, and young fully expanded leaves were selected for the measurements.

Gas Exchange Measurements and Rapid Freeze-Clamping of Leaves

Leaf gas exchange was measured in a chamber attached to a rapid freeze-clamping apparatus (Badger et al., 1984) using a portable gas exchange system (LI 6400, LI-COR, Lincoln, NE) as described in Ruuska et al. (1998). CO₂ assimilation was measured at an irradiance of 1,000 $\mu\text{mol quanta m}^{-2} \text{s}^{-1}$ at either 350 to 380 microbars (μbar) or 700

μbar CO₂ in air, and the leaf temperature was kept at 25°C. For the measurements conducted at 350 μbar , the leaf was stabilized for at least 40 min before it was rapidly freeze-clamped. For the 700- μbar CO₂ measurements a section of the same leaf was first kept at 350 μbar CO₂ in air, 1,000 $\mu\text{mol quanta m}^{-2} \text{s}^{-1}$ until stomatal opening was nearly complete (about 20 min), after which the incoming CO₂ partial pressure was increased to 700 μbar . The gas exchange characteristics were recorded after 30 to 40 min, and a leaf disc was freeze-clamped. Additional leaf discs were collected for chlorophyll and Cyt *f* measurements and GAPDH activity assays.

Enzyme Assays

For Rubisco assays, one-half of the freeze-clamped leaf disc (2.7 cm²) was homogenized in 1.4 mL of ice-cold CO₂-free extraction buffer containing 50 mM 4-(2-hydroxyethyl)-1-piperazineethanesulfonic acid (HEPES)-NaOH, pH 7.8, 1 mM Na-EDTA, 5 mM MgCl₂, 10 mM dithiothreitol (DTT), 1% (w/v) polyvinylpyrrolidone, and 1 mM phenylmethylsulfonyl fluoride (PMSF). The extract was centrifuged for 15 to 20 s (10,000g), and the initial activity of Rubisco was measured immediately at 25°C by adding a 10- μL aliquot of the supernatant into 262 μL of the reaction mixture containing 55 mM 4-(2-hydroxyethyl)-1-piperazinepropanesulfonic acid (HEPPS)-KOH, pH 8.0, 22 mM MgCl₂, 0.27 mM Na-EDTA, 13 mM NaH¹⁴CO₃ (specific radioactivity approximately 1,500 cpm/nmol), and 0.4 mM RuBP. Total activity was assayed after 10 μL of the supernatant was incubated at 25°C for 5 min in 55 mM HEPPS-KOH, pH 8.0, 22 mM MgCl₂, 0.27 mM Na-EDTA, and 14.5 mM NaH¹⁴CO₃. The assay was initiated by adding 0.4 mM RuBP. In both assays the reaction was terminated after 60 s with formic acid, samples were dried and acid-stable ¹⁴C was measured by liquid scintillation. The exact specific radioactivity of NaH¹⁴CO₃ was determined for each set of assays by measuring the amount of ¹⁴C rendered acid stable by allowing a reaction containing 10 nmol of RuBP (measured spectrophotometrically according to the method of He et al. [1997]) go to completion with excess Rubisco using the procedure described for total activity.

The Rubisco catalytic site concentration was determined by the stoichiometric binding of [¹⁴C]CPBP (an unresolved mixture of 2'-carboxy-D-arabinitol-1,5-bisphosphate and 2'-carboxy-D-ribitol-1,5-bisphosphate), and the carbamylation level was measured by exchanging loosely bound [¹⁴C]CPBP at non-carbamylated sites with an excess of [¹²C]CPBP (Butz and Sharkey, 1989) as described in Ruuska et al. (1998). The catalytic turnover rates were calculated by dividing the initial or total in vitro activities by the number of carbamylated or total Rubisco sites.

Total GAPDH activity was determined spectrophotometrically as described in Stitt et al. (1989) and Ruuska et al. (1998).

The activation state of chloroplast NADP-MDH was assayed according to the method of Scheibe and Stitt (1988) with minor modifications. One-half of a freeze-clamped leaf disc was extracted in 900 μL of ice-cold buffer (sparged with humidified nitrogen) containing 50 mM Na-acetate,

pH 6.0, 1% (w/v) bovine serum albumin (BSA), 4 mM DTT, 0.1% (w/v) Triton X-100, 0.5 mM benzamidine, 0.5 mM ϵ -aminocaproic acid, and 0.5 mM PMSF. The crude extract was centrifuged at 10,000g for 5 min at 4°C, and the initial activity of NADP-MDH was assayed immediately in a total volume of 1.5 mL containing 100 mM Tris-HCl, pH 8.0 (sparged with humidified nitrogen), 1 mM Na-EDTA, 1 mM DTT, 0.2 mM NADPH, and 100 μ L of supernatant.

The reaction was initiated by adding 2 mM oxaloacetic acid and the decline in A_{340} was monitored. Reductive activation of NADP-MDH was achieved by incubating an aliquot of the supernatant in 250 mM Tris-HCl, pH 9.0 (sparged with nitrogen), and 125 mM DTT under nitrogen atmosphere at room temperature for 15 min. Time course experiments confirmed that 15 min was sufficient to fully activate tobacco NADP-MDH. The low DTT concentration in the extraction buffer (4 mM) did not cause activation of the enzyme. NADP-MDH activities were corrected for the side activity of NAD-MDH, which was assumed to be 0.2% of the total NAD-MDH activity (Scheibe and Stitt, 1988; Grace and Logan, 1996). The total NAD-MDH activity was measured in 1.5 mL in 100 mM Tris-HCl, pH 8.0, 10 mM $MgCl_2$, 0.2 mM NADH, and 10 μ L of diluted supernatant. The reaction was initiated with 1 mM oxaloacetic acid (Scheibe and Stitt, 1988). With this procedure, activation levels below 5% were obtained from dark- or low-light-adapted tobacco.

Western-Blot Quantitation of Cyt *f* and Rubisco Activase Content

Anti-*bff* plants have been characterized previously by measuring the amount of FeS polypeptide in leaves by western blotting. In this study an antibody directed against the Cyt *f* protein was used (Barkan et al., 1986) because of its higher specificity. A close correlation between the amounts of FeS and Cyt *f* protein has been demonstrated (Anderson et al., 1997; Price et al., 1998), indicating that the content of the whole Cyt *bff* complex is reduced by the antisense construct. The western blotting and protein quantitation were performed as described previously (Price et al., 1995b). The amount of Rubisco activase in leaves was measured as in Mate et al. (1993).

Metabolite and Adenylate Assays

Extraction Procedure

One-half of the rapid-kill leaf disc was quickly weighed (while frozen) and ground into powder in a mortar cooled with liquid nitrogen. Five-hundred microliters of 5% (w/v) perchloric acid containing 10 mM EDTA was added and the mixture was homogenized until melted. The crude extract was transferred to a microcentrifuge tube and heated for 5 min in a 60°C water bath to inactivate nucleotide phosphohydrolase activity not destroyed by acid alone (Ikuma and Tetley, 1976; Biotto and Siegenthaler, 1994), cooled on ice, and centrifuged at 4°C for 10 min at 10,000g. An aliquot of

the supernatant was neutralized to pH 6.0 to 7.0 using 3 M K_2CO_3 and kept on ice before $KClO_4$ was removed by centrifugation at 10,000g for 10 min at 4°C. The sample was aliquoted, snap-frozen, and stored at -80°C.

Luminometric Determination of ATP and ADP

A sensitive luminometric procedure was chosen to enable all metabolites and adenylates to be measured with a single half-leaf disc derived from the freeze-clamping apparatus. ATP content was measured using a luminometer (TD 20/20, Turner Designs, Sunnyvale, CA) fitted with an autoinjector. The assay mixture contained reaction buffer (10 mM N-[2-hydroxy-1,1-Bis(hydroxymethyl)ethyl]-glycine-KOH [Tris-KOH], pH 7.75, 8.75 mM Mg-acetate, 0.5 mM EDTA, and 20 mM KCl) and diluted sample in a total volume of 80 μ L. The measurements were initiated by injecting 100 μ L of appropriately diluted luciferin/luciferase reagent (ATP Bioluminescence Assay Kit CLS II, Boehringer Mannheim/Roche, Basel, or ATP assay mix, Sigma Chemicals, St. Louis) into the assay mixture, and the total light signal emitted was integrated for 5 s after a 3-s delay. Internal standardization was carried out by measuring each sample twice, once alone and once with 10 pmol of ATP added (Wulff and Doppen, 1985).

For ADP determinations, 200 μ M phosphoenolpyruvate (PEP) was added to the reaction buffer. The enzymatic conversion of ADP to ATP was started by adding 0.2 unit of pyruvate kinase to each reaction mixture. After 25 min at room temperature, ATP was assayed by injecting the luciferin/luciferase reagent as described above. The internal standardization with ATP was the same as for the ATP assays.

Luminometric Determination of 3-Phosphoglycerate (PGA) and RuBP

We expanded the assay method of Lilley et al. (1985), which uses several glycolytic enzymes to convert PEP, 2-phosphoglycerate (2-PGA), and 3-phosphoglycerate (3-PGA) to pyruvate, coupled with stoichiometric conversion of ADP to ATP. A third step was incorporated in which Rubisco and $NaHCO_3$ were added to the assay mixture to convert RuBP to 3-PGA. Three separate assays were performed for each sample. First, the combined background amount of ATP, PEP, and 2-PGA were assayed by including enolase and pyruvate kinase in the assay mixture. In the second step, phosphoglycerate mutase was added and the sum of ATP, PEP 2-PGA, and 3-PGA was determined. Finally, by including Rubisco and $NaHCO_3$, the sum of RuBP, 3-PGA, ATP, PEP, and 2-PGA was measured. The actual amounts of 3-PGA and RuBP were then obtained by subtraction.

The metabolite assays were performed in the same manner as the ADP assays but with 3 μ M ADP and 5 mM $NaHCO_3$ substituted for PEP in the preliminary incubation buffer. The reaction for the measurement of [ATP + PEP + 2-PGA] was initiated by adding 0.4 unit of pyruvate kinase and 0.04 unit of enolase to the mixture. For assaying the

total amount of [3-PGA + ATP + 2-PGA + PEP], 0.003 unit of phosphoglycerate mutase was also included, and when measuring [RuBP + 3-PGA + ATP + 2-PGA + PEP], 0.008 unit of tobacco Rubisco purified according to the method of Servaites (1985) was also present. After 25 min, ATP produced was measured by injecting the luciferin/luciferase reagent as described above. The samples were diluted so that <20 pmol of ATP was produced. Internal standardization with ATP was the same as for the ATP assays.

For metabolite assays, 2,3-biphosphoglycerate-independent phosphoglycerate mutase was purified from wheat germ as described by Ruuska (1998) using methods based on those of Grisolia and Carreras (1975), Leadlay et al. (1977), Smith and Hass (1985), and Grana et al. (1989), with an additional step to remove adenylate kinase by adsorption to a HiTrap Blue (Pharmacia Biotech, Piscataway, NJ) affinity column.

It was noted by Lilley et al. (1985) (and also by us) that there is a background formation of ATP in this system due to ATP production from ADP by traces of adenylate kinase present in the pyruvate kinase and tobacco Rubisco preparations. The effect of this background activity was reduced by keeping the substrate ADP concentration and the amounts of the coupling enzymes as low as possible. With these precautions, the background ATP content measured in the absence of metabolite samples was 0.5 to 1 pmol per assay.

Recovery Tests

The recoveries of adenylates and metabolites were checked by adding 20 to 30 nmol of ATP, ADP, 3-PGA, and RuBP (together or separately) to perchloric acid extracts of leaf discs before assay by the above procedures. The exact concentrations of the added adenylates or metabolites were determined by spectrophotometric assays. ATP was determined with phosphoglycerate kinase-glyceraldehyde phosphate dehydrogenase and ADP with pyruvate kinase-lactate dehydrogenase (Bergmeyer and Grassl, 1985). 3-PGA and RuBP were measured as described by He et al. (1997). The recoveries (averages \pm SE) were: ATP, 99% \pm 2% ($n = 6$); ADP, 92% \pm 4% ($n = 3$); 3-PGA, 86% \pm 7% ($n = 4$); and RuBP, 98% \pm 4% ($n = 5$).

RESULTS

CO₂ Assimilation Rates

Individual tobacco plants with a variety of Cyt *f* contents were screened initially by measuring chlorophyll fluorescence (Price et al., 1995b). Plants with Cyt *f* contents ranging between 60% to 5% of the average wild-type level were obtained (Fig. 1, A and C). These plants had to be grown under low light to minimize the instability of the antisense phenotype (Price et al., 1995b). However, the extended daylength ensured that CO₂ assimilation rates of the

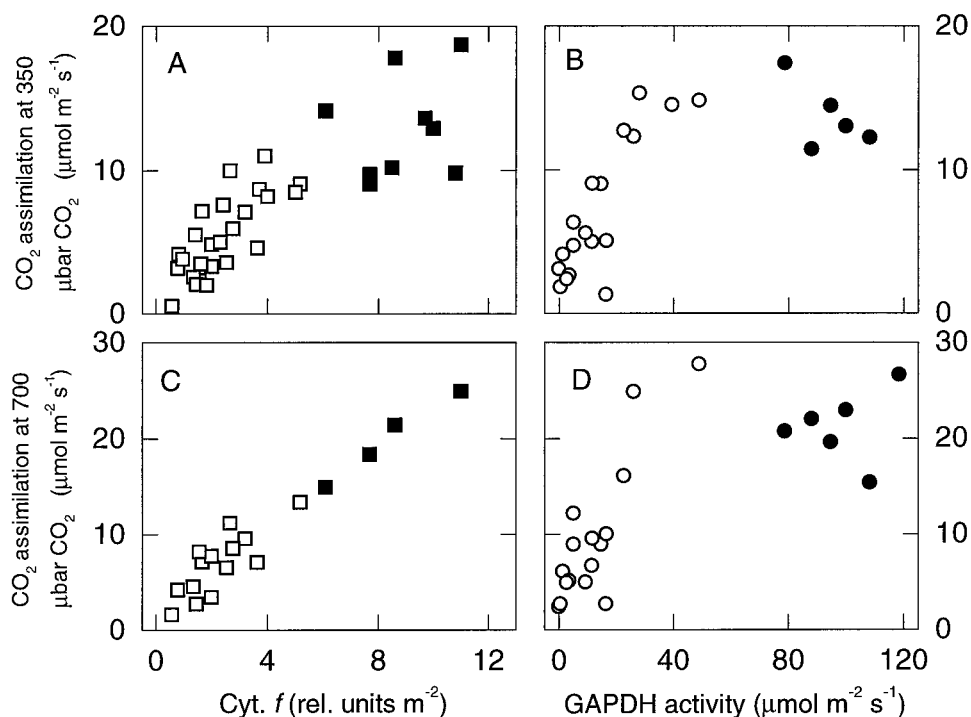


Figure 1. CO₂ assimilation rates of low-light-grown wild-type tobacco plants (■) and transgenic tobacco plants with a variety of Cyt *b/f* contents (□) (A and C), and greenhouse-grown wild-type (●) and transgenic tobacco plants with different activities of GAPDH (○) (B and D) were measured using the combined gas exchange and rapid-kill procedure described by Badger et al. (1984). Measurements were conducted at an irradiance of 1,000 $\mu\text{mol quanta m}^{-2} \text{s}^{-1}$, a CO₂ partial pressure of 350 μbar or 700 μbar , 21% (v/v) O₂, and a leaf temperature of 25°C. Leaves were kept under these conditions for at least 40 min before the CO₂ assimilation rate was recorded and a leaf disc was rapidly freeze-clamped.

growth-cabinet-grown wild-type plants were similar to the wild-type plants grown together with the anti-GAPDH plants in the greenhouse (Fig. 1, A and B). The CO₂ assimilation rate decreased when the amount of Cyt *f* was reduced (Fig. 1A). The most severely effected anti-*b/f* plants had assimilation rates below 3 μmol m⁻² s⁻¹, while the average rate for the wild-type plants was 12.8 μmol m⁻² s⁻¹. When the CO₂ assimilation rates were measured at 700 μbar CO₂, the relationship between leaf Cyt *f* content and assimilation rate at high light became strikingly linear (Fig. 1C), whereas at 350 μbar CO₂ the relationship was more curvilinear (Fig. 1A).

Anti-GAPDH plants had a variety of GAPDH activities from about 50% to less than 5% of wild-type level and assimilation rates ranging to below 10% of the average wild-type rate when measured at 350 μbar CO₂ (Fig. 1, B and D). There was no effect on the CO₂ assimilation rate at 350 μbar CO₂ until GAPDH activity was reduced to below 30% of wild-type level. The relationship between the assimilation rate and GAPDH activity was similar at 700 and 350 μbar CO₂.

The Contents of Rubisco, 3-PGA, and RuBP

The average Rubisco contents of leaves are presented in Table I. Rubisco content was on average 25% lower in low-light-grown plants than in greenhouse-grown plants. The soluble protein content, on a leaf-area basis, was also lower in low-light-grown plants (data not shown). Consequently, the Rubisco content as a fraction of soluble proteins was similar at the two light intensities, being on average, 28% ± 2% for all low-light grown plants and 31% ± 3% for all greenhouse-grown plants. The decrease in either the Cyt *b/f* content or GAPDH activity did not cause significant changes in the content of Rubisco of the leaves compared with their respective control plants (Table I).

The growth conditions had a strong impact on the RuBP content of wild-type leaves. When measured from leaves kept at 1,000 μmol quanta m⁻² s⁻¹, the low-light-grown wild-type plants had approximately 50% less RuBP than greenhouse-grown wild-type plants, regardless of the measuring CO₂ concentration (Table I). Because both RuBP and Rubisco contents were lower in low-light-grown wild-type plants, the ratio of RuBP to Rubisco sites was only slightly less than in the greenhouse-grown wild-type plants. The

reduction in both the Cyt *b/f* content and GAPDH activity reduced the contents of RuBP in the transgenic plants. When measured at 350 μbar CO₂, the RuBP content declined to close to the Rubisco site concentration in both plant types, but not below it. The amount of 3-PGA was comparable to wild-type levels in both of the antisense plant types at 350 μbar CO₂. As a consequence, the RuBP/3-PGA ratio fell significantly below wild-type levels in both transgenic plant types.

When the leaves were exposed to 700 μbar CO₂, the RuBP content decreased in all plants (Table I). This was associated with an increase in 3-PGA pool sizes, so the RuBP/3-PGA ratio was lower than at 350 μbar CO₂ in all plants. Despite the decrease in RuBP content at elevated CO₂, the ratio between RuBP and Rubisco sites remained above 1 in most of the wild-type and anti-*b/f* plants. At 700 μbar CO₂, however, the RuBP content in almost all anti-GAPDH plants decreased below the Rubisco site concentration, and the average RuBP per site ratio was 0.72.

Whole-Leaf Adenylate Contents

The amounts of ATP and ADP in the leaves were measured to assess changes in the adenylate pools due to the shifted balance between ATP production and consumption in the chloroplasts (Fig. 2; Table II). The reduction in Cyt *f* content did not affect the whole-leaf adenylate content: both the total amounts of ATP and ADP and the ratio between the two remained similar to wild-type levels, even in the most severe antisense plants (Fig. 2, A, C, E, and G). On average, the low-light grown plants had 14.8 ± 2 μmol ATP and 10.9 ± 1 μmol ADP m⁻² and the ratio of ATP/ADP was 1.43 ± 0.1. In contrast, when the activity of GAPDH was reduced below 50% of the wild-type level, the amount of ATP increased and, simultaneously, ADP content decreased. This led to an approximately 2-fold rise in the ATP/ADP ratio compared with wild-type plants (on average, 1.55 ± 0.34 in the wild type and up to 3.1 in the most severe anti-GAPDH plants), whereas the sum of ATP + ADP remained constant, being 44 ± 6 μmol m⁻² in all greenhouse-grown plants (Fig. 2, B, D, F, and H).

When the CO₂ concentration was increased to 700 μbar, it had little effect on the ATP/ADP ratios in the wild-type and anti-*b/f* tobacco plants compared with the ratios at 350 μbar (Table II). There was also no difference in the ATP/

Table I. Contents of Rubisco, RuBP, and 3-PGA in leaves of anti-*b/f*, anti-GAPDH, and the respective wild-type (WT) tobacco plants

The measurements were made at 350 or 700 μbar CO₂ at an irradiance of 1,000 μmol quanta m⁻² s⁻¹ and a leaf temperature of 25°C. The values are averages ± SE, with the number of replicates indicated in the parentheses.

	Growth-Cabinet-Grown Plants				Greenhouse-Grown Plants			
	350 μbar CO ₂		700 μbar CO ₂		350 μbar CO ₂		700 μbar CO ₂	
	WT (n = 4)	Anti- <i>b/f</i> (n = 13)	WT (n = 4)	Anti- <i>b/f</i> (n = 13)	WT (n = 4)	Anti-GAPDH (n = 9)	WT (n = 4)	Anti-GAPDH (n = 8)
Rubisco sites (μmol m ⁻²)	15.4 ± 0.6	13.0 ± 1.3	13.8 ± 0.6	13.5 ± 1.5	20.0 ± 1.9	19.8 ± 1.7	21.0 ± 1.2	19.2 ± 2.0
RuBP (μmol m ⁻²)	72 ± 8	29 ± 4	25 ± 8	20 ± 2	130 ± 7	42 ± 18	39 ± 4	14 ± 3
3-PGA (μmol m ⁻²)	68 ± 8	62 ± 7	119 ± 5	75 ± 8	77 ± 11	92 ± 10	158 ± 9	135 ± 20
RuBP/3-PGA (mol mol ⁻¹)	1.1 ± 0.2	0.44 ± 0.04	0.20 ± 0.05	0.26 ± 0.04	1.78 ± 0.25	0.43 ± 0.12	0.25 ± 0.04	0.11 ± 0.06
RuBP/Rubisco sites (mol mol ⁻¹)	4.7 ± 0.5	2.2 ± 0.3	1.8 ± 0.6	1.4 ± 0.2	6.4 ± 0.4	2.0 ± 0.6	1.9 ± 0.2	0.72 ± 0.4

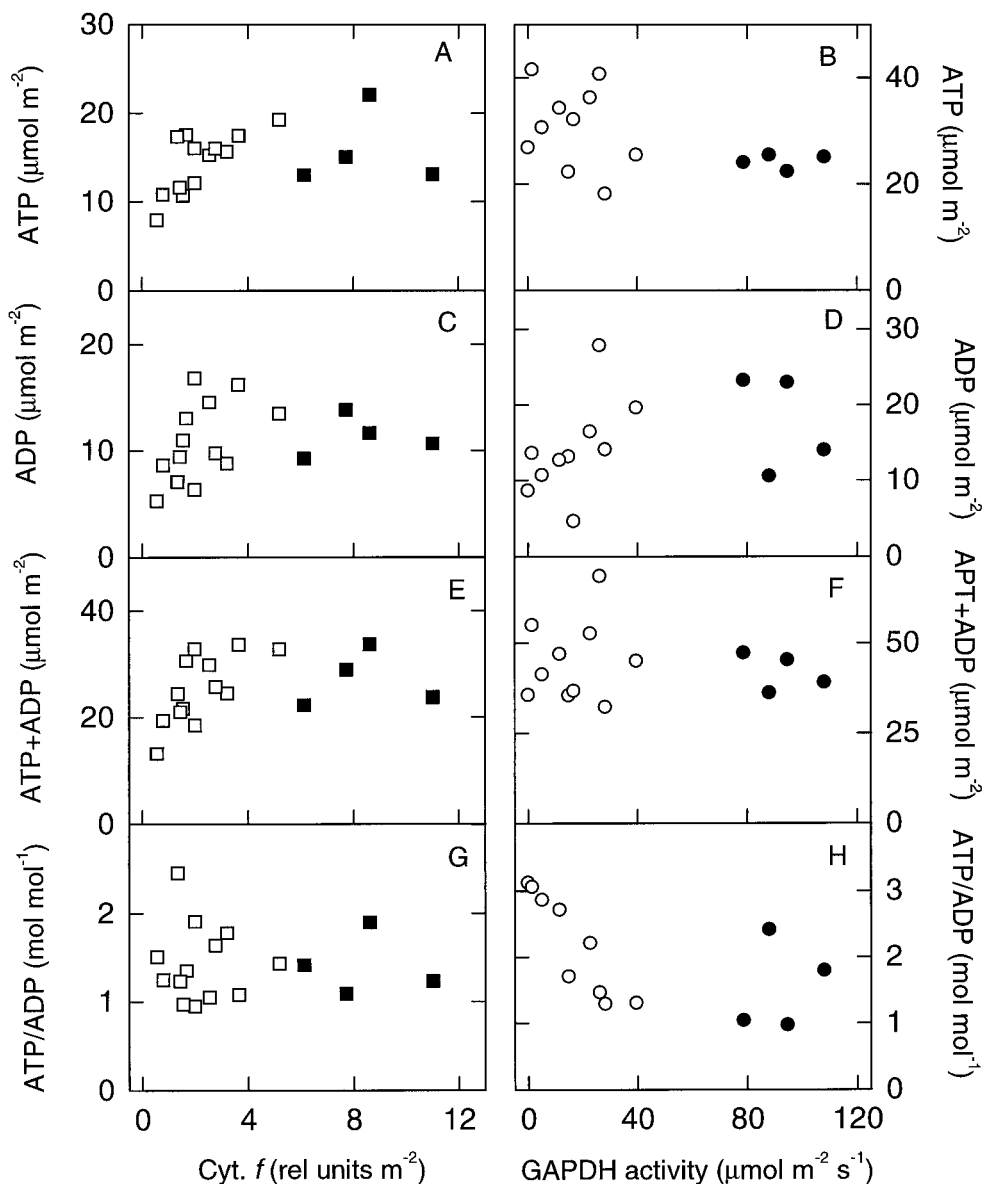


Figure 2. Whole-leaf ATP (A and B) and ADP (C and D) concentrations, the sum of ATP + ADP (E and F), and the ATP/ADP ratio (G and H) in leaves of wild-type, anti-*b/f*, and anti-GAPDH tobacco plants measured at 350 $\mu\text{bar CO}_2$. Leaves were freeze-clamped after the gas-exchange measurements at 350 $\mu\text{bar CO}_2$ shown in Figure 1. Symbols are as in Figure 1. These data are summarized in Table I and compared with similar measurements at 700 $\mu\text{bar CO}_2$.

Table II. Leaf adenylate contents in leaves of anti-*b/f*, anti-GAPDH, and the respective wild-type (WT) tobacco plants

The measurements were made at 350 or 700 $\mu\text{bar CO}_2$ at an irradiance of 1,000 $\mu\text{mol quanta m}^{-2} \text{s}^{-1}$ and a leaf temperature of 25°C. The values are averages \pm SE, with the number of replicates indicated in parentheses.

	Growth-Cabinet-Grown Plants				Greenhouse-Grown Plants			
	350 $\mu\text{bar CO}_2$		700 $\mu\text{bar CO}_2$		350 $\mu\text{bar CO}_2$		700 $\mu\text{bar CO}_2$	
	WT (n = 4)	Anti- <i>b/f</i> (n = 13)	WT (n = 4)	Anti- <i>b/f</i> (n = 13)	WT (n = 4)	Anti-GAPDH (n = 10)	WT (n = 3)	Anti-GAPDH (n = 9)
ATP ($\mu\text{mol m}^{-2}$)	15.8 \pm 2.1	14.4 \pm 4.2	13.5 \pm 1.8	16.0 \pm 1.2	24.0 \pm 0.7	30.8 \pm 2.4	31.4 \pm 3.1	31.8 \pm 3.2
ADP ($\mu\text{mol m}^{-2}$)	11.3 \pm 1.0	10.8 \pm 1.0	12.3 \pm 1.3	12.5 \pm 0.8	17.7 \pm 3.2	14.1 \pm 2.0	17.7 \pm 2.6	21.2 \pm 4.1
ATP+ADP ($\mu\text{mol m}^{-2}$)	27.4 \pm 2.6	25.2 \pm 1.8	25.9 \pm 3.0	28.5 \pm 1.7	41.9 \pm 2.6	44.9 \pm 3.6	49.1 \pm 1.9	50.9 \pm 5.9
ATP/ADP (mol mol^{-1})	1.41 \pm 0.18	1.43 \pm 0.12	1.10 \pm 0.11	1.31 \pm 0.10	1.55 \pm 0.34	2.67 \pm 0.53	1.66 \pm 0.3	1.70 \pm 0.23

ADP ratio between the low-light-grown wild-type and anti-*b/f* plants at 700 $\mu\text{bar CO}_2$. At elevated CO_2 , however, the average ATP/ADP ratio in the anti-GAPDH plants decreased and become similar to the wild-type ratio. It is worth noting that at 700 $\mu\text{bar CO}_2$ the ATP/ADP ratio was higher in the anti-GAPDH plants with the lowest GAPDH activity than in wild-type plants and transgenic plants with intermediate GAPDH activity (data not shown).

NADP-MDH Activation State

The activation state of the chloroplast NADP-MDH was measured as the ratio between the initial (non-activated) activity and the total activity (after 15 min of reductive activation, see Scheibe and Jacquot [1983]) from leaf samples collected from 350 $\mu\text{bar CO}_2$ and 1,000 $\mu\text{mol quanta m}^{-2} \text{s}^{-1}$. The activation state decreased dramatically when the Cyt *b/f* content was reduced (Fig. 3A), indicating a

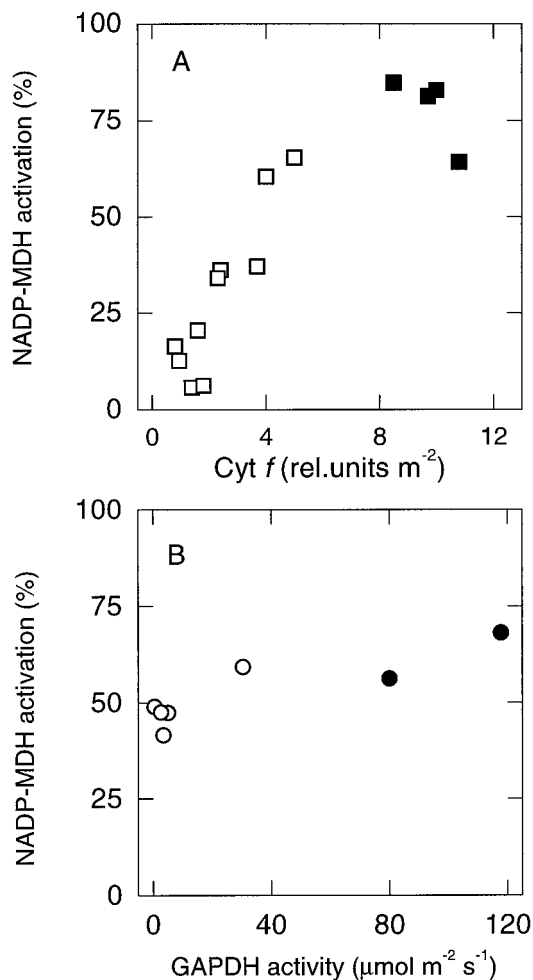


Figure 3. NADP-MDH activation levels in the leaves of wild-type, anti-*b/f*, and anti-GAPDH tobacco plants measured at 350 $\mu\text{bar CO}_2$. Symbols, measuring conditions, and sampling were as in Figures 1 and 2. The mean total activities were 11.6 ± 0.04 and 10.4 ± 0.15 $\mu\text{mol m}^{-2} \text{s}^{-1}$, respectively, for anti-*b/f* and their wild-type plants and 15.1 ± 0.2 and 18.5 ± 0.3 $\mu\text{mol m}^{-2} \text{s}^{-1}$, respectively, for anti-GAPDH and their wild-type plants.

strong decline in the NADPH/NADP⁺ ratio. At 1,000 $\mu\text{mol quanta m}^{-2} \text{s}^{-1}$ the NADP-MDH activation in low-light-grown wild-type plants was $76\% \pm 4\%$, and decreased to 5% in the most severely affected antisense plants. The reduction in the activation level was due to a decrease in the initial activity of the enzyme (data not shown). In contrast, lowered GAPDH activities did not affect the NADP-MDH activation level compared with the wild-type plants (Fig. 3B). The average activation level in greenhouse-grown wild-type and anti-GAPDH plants was $53\% (\pm 4\%)$ when measured at 1,000 $\mu\text{mol quanta m}^{-2} \text{s}^{-1}$.

Rubisco Carbamylation State and in Vitro Activities

At high light and 350 $\mu\text{bar CO}_2$, the carbamylation state of Rubisco was high (80%) in all wild-type and anti-GAPDH plants (Fig. 4B; Table III). However, as the amount of Cyt *b/f* content reduced, the Rubisco carbamylation status declined, being less than 50% in the most severe anti-*b/f* plants (Fig. 4A). In Figure 4, C to F, the catalytic turnover rates of Rubisco sites are presented as a proportion of the average rate in control plants, and the mean values are given in Table III. There was no significant difference in the turnover rate of the carbamylated sites (initial activity per carbamylated sites) in either of the transgenic plant types compared with control plants. The total turnover rates (total activity per total sites) in anti-GAPDH plants were identical to controls as well. Nevertheless, in anti-*b/f* plants there was a significant decrease in the total activity per total Rubisco sites as the Cyt *f* content declined, such that the most severe anti-*b/f* plants had about half the turnover rate of the control plants. Similar results were obtained when the leaves were measured at 700 $\mu\text{bar CO}_2$ (Table III).

RuBP Content and Rubisco Turnover Rates in Vivo

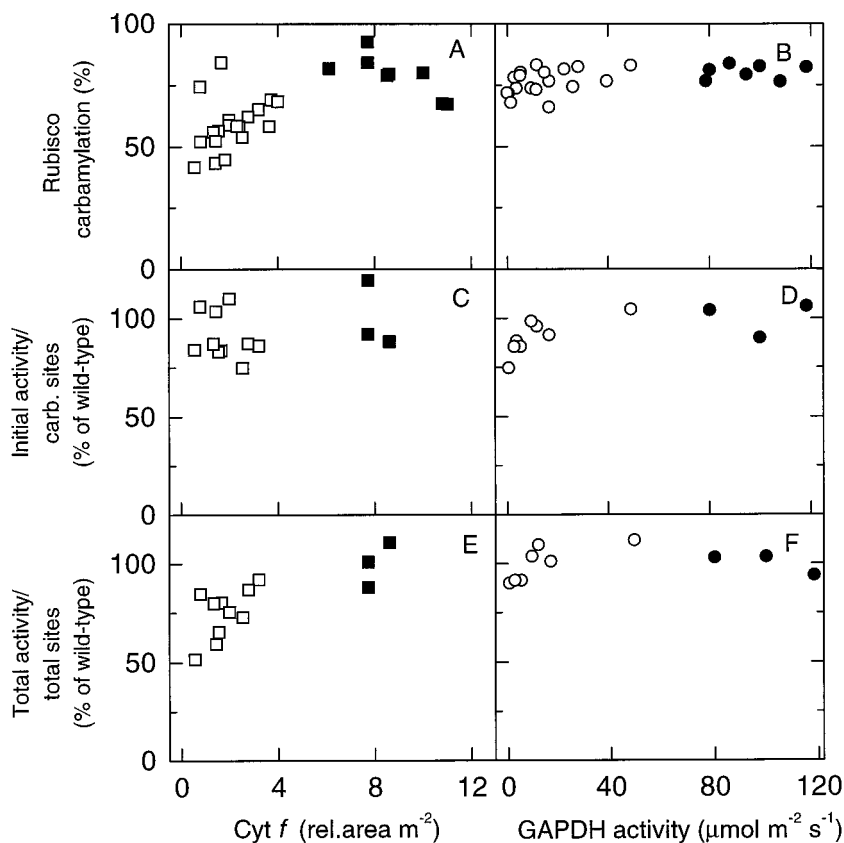
Figure 5, A and B, illustrates the changing relationships between RuBP and Rubisco sites in both anti-*b/f* and anti-GAPDH plants. As summarized in Table I, the RuBP/Rubisco site ratio at 350 $\mu\text{bar CO}_2$ declined from wild-type levels (between 4 and 7) down to around 1. As the RuBP content declines, the in vivo turnover rates of Rubisco decrease due to substrate limitation. Figure 5, C and D, present the in vivo turnover rates of carbamylated Rubisco sites (calculated from the gas exchange measurements and Rubisco assays) at 350 $\mu\text{bar CO}_2$. The average rates were $1.18 \pm 0.08 \text{ s}^{-1}$ and $0.97 \pm 0.06 \text{ s}^{-1}$ for the low-light and greenhouse-grown wild-type plants, respectively. In the most severe transgenic plants with the lowest RuBP content, the turnover rates were more than 50% lower than in the wild types. Figure 5, E and F, shows the in vivo turnover rates of carbamylated Rubisco sites as a function of RuBP content.

DISCUSSION

CO_2 Assimilation Decreases in Anti-*b/f* and Anti-GAPDH Plants

The decrease in Cyt *b/f* content caused the CO_2 assimilation rate to decline (Fig. 1, A and C), as demonstrated

Figure 4. Carbamylation state of Rubisco (A and B), initial in vitro activity of Rubisco per carbamylated (carb.) Rubisco sites (C and D), and total in vitro activity of Rubisco per total Rubisco sites (E and F) in leaves of wild-type, anti-*b/f*, and anti-GAPDH tobacco plants. Leaves were freeze-clamped after the gas-exchange measurements at 350 μbar CO_2 (shown in Fig. 1). The activity results (C–F) are expressed as a percentage of the average wild-type activities; mean values are given in Table II, which compares them with analog values measured at 700 μbar . The symbols are as in Figure 1.



earlier (Price et al., 1995b, 1998). At 350 μbar CO_2 , the relationship between the Cyt *b/f* content and the CO_2 assimilation rate was curvilinear, but as the leaves were exposed to 700 μbar CO_2 , the relationship became linear. This was expected, since at high CO_2 and high light CO_2 assimilation is limited solely by the electron transport capacity (Farquhar et al., 1980). The curvilinear relationship between the assimilation rate and the Cyt *b/f* content at 350 μbar CO_2 indicates that at ambient CO_2 , wild-type plants are close to the transition from Rubisco carboxylation-limitation to RuBP-regeneration limitation (von Caemmerer and Farquhar, 1981). As reported previously (Price et al., 1995a), the activity of GAPDH could be reduced to about 30% of the average wild-type activity before the CO_2 assimilation rates at 350 μbar CO_2 were affected. The ac-

tivity of GAPDH does not appear to be limiting for photosynthesis even at elevated CO_2 because, again, the CO_2 assimilation rates decreased only in plants with less than 30% of the wild-type GAPDH activity.

As reported previously (Price et al., 1995a, 1998), the decreased CO_2 assimilation rate in both anti-*b/f* and anti-GAPDH plants was associated with reduced RuBP concentration (Table I; Fig. 5, A and B). In anti-GAPDH plants, the reason for the lowered RuBP concentration was straightforward: the reduced amount of GAPDH forms a bottleneck in the regeneration pathway. In anti-*b/f* plants, however, there are two reasons. First, the electron transport rate has decreased in these plants, leading to decreased rate of ATP and NADPH synthesis. Second, there is a possibility that, in anti-*b/f* plants, the ferredoxin-thioredoxin-mediated

Table III. Rubisco carbamylation (carb.) and in vitro activities (act. of) anti-*b/f*, anti-GAPDH, and the respective wild-type tobacco plants

The measurements were made at 350 or 700 μbar CO_2 at an irradiance of 1,000 μmol quanta m^{-2} s^{-1} and a leaf temperature of 25°C. The values are averages \pm SE, with the number of replicates indicated in parentheses. Init., Initial.

	Growth-Cabinet-Grown Plants				Greenhouse-Grown Plants			
	350 μbar CO_2		700 μbar CO_2		350 μbar CO_2		700 μbar CO_2	
	WT	Anti- <i>b/f</i>	WT	Anti- <i>b/f</i>	WT	Anti-GAPDH	WT	Anti-GAPDH
Carbamylation (%)	79 \pm 3 (n = 9)	58 \pm 2 (n = 20)	74 \pm 4 (n = 5)	63 \pm 3 (n = 12)	80 \pm 1 (n = 7)	76 \pm 1 (n = 18)	79 \pm 2 (n = 7)	77 \pm 1 (n = 18)
Init. act./carb. sites (s^{-1})	2.56 \pm 0.25 (n = 3)	2.32 \pm 0.09 (n = 10)	2.77 (n = 2)	2.41 \pm 0.13 (n = 9)	3.76 \pm 0.19 (n = 3)	3.37 \pm 0.13 (n = 8)	4.03 \pm 0.12 (n = 3)	3.57 \pm 0.12 (n = 9)
Total act./total. sites (s^{-1})	2.46 \pm 0.16 (n = 3)	1.85 \pm 0.10 (n = 10)	2.43 \pm 0.20 (n = 3)	1.96 \pm 0.09 (n = 9)	2.77 \pm 0.09 (n = 3)	2.86 \pm 0.15 (n = 10)	3.06 \pm 0.11 (n = 3)	2.77 \pm 0.08 (n = 8)

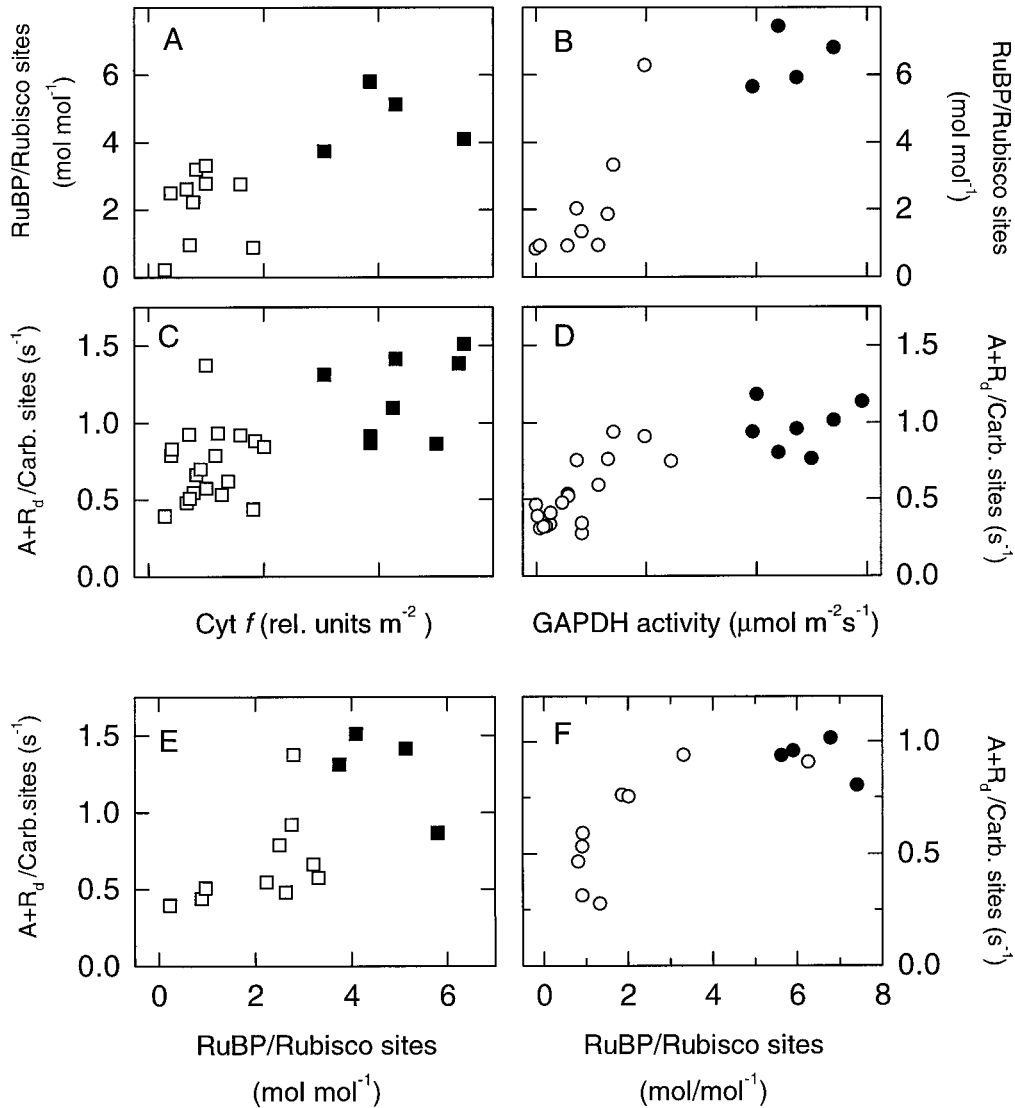


Figure 5. Ratio between RuBP and Rubisco sites (A and B) and the gross CO₂ assimilation rate per carbamylated (Carb.) Rubisco sites (C and D) and the relationship between gross CO₂ assimilation rate per carbamylated Rubisco site and the ratio between RuBP and Rubisco sites (E and F) in leaves of wild-type, anti-*b/f*, and anti-GAPDH tobacco plants. The gross CO₂ assimilation rates were calculated as $A + R_d$, where A is the CO₂ assimilation at 350 μbar CO₂ and R_d the dark respiration rate. Leaves were freeze-clamped after the gas-exchange measurements at 350 μbar CO₂ shown in Figure 1. The symbols are as in Figure 1.

activation of some of the PCR cycle enzymes has also decreased, further impairing the RuBP regeneration capacity. This assumption is supported by the large decrease in NADP-MDH activation state (Fig. 3A), which indicates a severe limitation of the NADPH synthesis and ferredoxin reduction, as discussed below.

At high CO₂ and high light, CO₂ assimilation in C₃ plants is determined by the RuBP regeneration rate. The transfer to elevated CO₂ decreased the RuBP pool sizes in all plants (Table I), but the RuBP content in most anti-*b/f* plants and all wild-type plants remained above the Rubisco site concentration. This is similar to previous studies on the response of chloroplast metabolites to changes in CO₂ showing that even at high CO₂, RuBP contents tend to exceed the

Rubisco site concentration (Badger et al., 1984; Dietz and Heber, 1984; von Caemmerer and Edmondson, 1986; Seemann et al., 1987). The RuBP pool sizes were only reduced below the Rubisco site concentration in the anti-GAPDH plants when exposed to 700 μbar CO₂. However, it should be kept in mind that, *in vivo*, the conditions in the chloroplast might be such that the maximal carboxylation efficiency requires RuBP concentrations well above the Rubisco site concentrations. Assuming that the Rubisco site concentration in the chloroplasts is 2 mM and the K_m for RuBP is 0.2 mM (allowing for competition by other phosphorylated compounds, but ignoring chelation by Mg²⁺), the approximate fractional activity of Rubisco is 0.95 when the RuBP/site ratio equals 2, and decreases to 0.75 when

this ratio reaches 1 (for details, see Ruuska et al. [1998]). Reduction of the free RuBP concentration by sequestration with divalent metals will reduce activity further.

Whole-Leaf ATP/ADP Does Not Change in Anti-*b/f* Plants, But the Activation of NADP-MDH Decreases

The balance between chloroplast electron transport and carbon assimilation, and therefore the production and consumption of ATP and NADPH, has been altered in opposite directions in anti-*b/f* and anti-GAPDH plants. The energy status of the leaves was studied by measuring whole-leaf adenylate levels. In addition, the activation state of the chloroplast NADP-MDH was measured and used as an indicator of the stromal NADPH/NADP⁺ ratio (Scheibe and Jacquot, 1983; Harbinson et al., 1990; Foyer, 1993).

The adenylate ratios in anti-*b/f* plants did not differ from wild-type plants irrespective of the CO₂ conditions (Table II). However, the severely decreased activation state of NADP-MDH in these plants (Fig. 3A) suggests that the rate of linear electron transport, and presumably also proton translocation, were reduced markedly. Chlorophyll fluorescence measurements have shown that the transthylakoid pH gradient is low in anti-*b/f* plants (Price et al., 1995b). Since only the whole-leaf adenylates were measured, it is possible that the cytosolic and mitochondrial pools may have masked the changes in the chloroplast ATP/ADP ratio. In a study conducted with protoplasts of wheat leaves, it was found that 47% of the total adenylates were located in the chloroplasts; 44% were located in the cytosol and 9% in the mitochondria (Stitt et al., 1982). The ATP/ADP ratio in the cytosol is higher than that in the chloroplasts, whether measured in the light or the dark, because ATP is transported there from chloroplasts and mitochondria (Stitt et al., 1982; Gardeström and Wigge, 1988; Heineke et al., 1991).

The observed reduction in the activation level of NADP-MDH in anti-*b/f* plants (Fig. 3A) resembles the results of Harbinson et al. (1990) and Krall et al. (1995). These authors measured NADP-MDH activation in leaves at different light intensities and noted a strong correlation between light intensity, electron transport rate, and NADP-MDH activation. The low activation state of NADP-MDH in anti-*b/f* plants indicates that the reduction state of the stromal NADP⁺ pool is significantly lowered. Decreased NADPH/NADP⁺ ratio has two main implications for carbon fixation. First, the lack of reducing equivalents limits the function of the PCR cycle and RuBP regeneration. Second, the low stromal reduction status reduces the activity of the chloroplast ferredoxin-thioredoxin pathway, and therefore the enzymes regulated by this system (for example Fru 1,6-bisphosphatase) are likely to be less active (Holfgreffe et al., 1997). The decreased activity of the PCR cycle enzymes may explain why the ATP/ADP ratio did not change in anti-*b/f* plants. The consumption of ATP by the PCR cycle may be severely restricted, thus compensating for the decreased rate of ATP synthesis. The same mechanism may also explain why light intensity generally has little effect on leaf adenylate levels (Dietz and Heber, 1984; Brooks et al., 1988a; Sage et al., 1990).

The activation level of NADP-MDH in the most severe anti-*b/f* plants at high light (Fig. 3A) resembles that seen in wild-type plants in darkness or very low light (data not shown), suggesting that *b/f* complex depletion impairs perception of the light signal by the thioredoxin pathway. When leaves were exposed to 1,000 $\mu\text{mol quanta m}^{-2} \text{s}^{-1}$, NADP-MDH in the low-light-grown wild-type plants activated to over 80%. This activation level is high compared with, for example, 35% in pea leaves measured in air and 1,000 $\mu\text{mol quanta m}^{-2} \text{s}^{-1}$ (Harbinson et al., 1990) or 53% in the greenhouse-grown wild-type and anti-GAPDH plants (Fig. 3B), which experienced growth light intensities close to measuring conditions. Greenhouse-grown plants had about 1.5 times greater total NADP-MDH activities (on an area basis) than low-light-grown plants (legend to Fig. 3), and this greater capacity may explain the different activation states observed in wild-type plants.

ATP/ADP Increases in Anti-GAPDH Plants But Not the Activation of NADP-MDH

The increase in the whole-leaf ATP/ADP ratio in anti-GAPDH plants at 350 $\mu\text{bar CO}_2$ (Fig. 2H) is comparable to the observations of other transgenic tobacco plants with impaired capacity for carbon assimilation, due to either the reduced amount of Rubisco (Quick et al., 1991) or of phosphoribulokinase (Paul et al., 1996). This effect of decreased carbon fixation capacity on the adenylate pools is analogous to the increase in ATP/ADP ratio when photosynthesis is limited by low CO₂ (Gardeström, 1987; Gilmore and Björkman, 1994), since the majority of ATP synthesized in chloroplasts is used in carbon metabolism. This was clearly the case in the anti-GAPDH plants, since increasing the CO₂ concentration caused the average ATP/ADP ratio to decline to close to wild-type levels (Table II).

Interestingly, the reduction state of the stromal NADP⁺ pool at 350 $\mu\text{bar CO}_2$ (estimated from the NADP-MDH activation level, Fig. 3B) in anti-GAPDH plants was similar to the wild-type plants. It might be expected to rise in the antisense plants with decreased capacity to use reducing equivalents in carbon fixation. These results are comparable to data obtained by Lauerer et al. (1993), who measured the activation state of NADP-MDH at growth irradiance in plants with reduced amounts of Rubisco. The maintenance of a wild-type-like NADPH/NADP⁺ ratio in anti-GAPDH plants indicates that PSII efficiency is well regulated in these plants, as had previously been demonstrated with measurements of chlorophyll fluorescence (Price et al., 1995a). Transport of reducing equivalents from chloroplasts to cytosol via the "malate shuttle" (Scheibe, 1987) may contribute to this regulation.

Reduction in the Electron Transport Capacity Affects Rubisco in Anti-*b/f* Plants

Carbamylation

The Rubisco carbamylation state in all wild-type and anti-GAPDH plants was on an average 80% at 350 $\mu\text{bar CO}_2$ and high light (Fig. 4, A and B; Table II), which is

typical for tobacco (Mate et al., 1993, 1996; Price et al., 1995a). However, the carbamylation level of Rubisco decreased when the amount of Cyt *b/f* was reduced (Fig. 4A), as previously reported (Price et al., 1998). The reason for the low carbamylation state could be that conditions in the chloroplasts are such that they directly inhibit the carbamylation process, or the decreased carbamylation could be mediated by Rubisco activase. It is possible that the stromal pH is lower in anti-*b/f* plants due to restricted electron transport and reduced transthylakoid proton gradient. The low pH can impair the carbamylation process, perhaps in concert with a reduction in the concentration of free Mg^{2+} in the stroma, as discussed previously (Price et al., 1998). However, the stromal buffering capacity is quite high (estimated as 30 mM), which should prevent large changes in pH (Hauser et al., 1995a, 1995b).

Alternatively, the decrease in carbamylation of Rubisco in anti-*b/f* plants is somewhat similar to the effect of reduced Rubisco activase content (Mate et al., 1993, 1996). However, the amount of Rubisco activase was the same in wild-type and anti-*b/f* plants (data not shown). This raises the interesting possibility that the activity of activase may be reduced in anti-*b/f* plants. The restriction in electron transport could decrease the stromal ATP/ADP ratio, which could inhibit the activase function. The decrease in carbamylation in anti-*b/f* plants would then be analogous to the suggested mechanism for Rubisco deactivation observed in phosphorus-depleted plants, in which ATP synthesis is limited by a lack of inorganic phosphate (Brooks et al., 1988b; Sharkey, 1990).

However, as discussed above, the ATP/ADP ratio in the anti-*b/f* plants was similar to the wild-type plants (Table II). There are several studies suggesting that, although Rubisco activase needs ATP to function, changes in the stromal ATP/ADP ratio may not be the only means by which activase activity and Rubisco carbamylation are modulated. Brooks et al. (1988a) suggested that the minimal changes in the stromal ATP/ADP ratio that occur when irradiance is varied are insufficient to account for the observed changes in Rubisco activation. Studies by Campbell and Ogren (1990a, 1990b, 1992) suggested that activase senses the light intensity via the electron transport rate through PSI rather than through stromal adenylates, and that the presence of a ΔpH is also required. Our results agree with this notion: the decrease in Rubisco carbamylation in anti-*b/f* plants can be interpreted as a consequence of activase being unable to detect the light signal.

The low carbamylation in anti-*b/f* plants was remarkably similar to the decrease in carbamylation in wild-type tobacco leaves when the light intensity was reduced (data not shown): in both cases the carbamylation decreased from a maximum of 80% down to 40%. In anti-GAPDH plants, on the other hand, in which the photosynthetic electron transport rate was also reduced, the carbamylation state remained high (Fig. 4, Price et al., 1995a). These plants have a high ΔpH (Price et al., 1995a), a high ATP/ADP ratio (Table II), and the degree of reduction of pyridine nucleotides remained similar to that of wild-type plants (Fig. 3).

Our results indicate that the light regulation of Rubisco activase in vivo is not mediated by the stromal ATP/ADP

ratio or the electron transport rate per se, but rather by some manifestation of the balance between electron transport rate and the consumption of its products. Possibilities include the ΔpH or the degree of reduction of the acceptor side of PSI. The mechanism by which activase activity could respond to these factors is unclear. A recent report of regulation of activase activity via the thioredoxin pathway (Zhang and Portis, 1999) would provide a ready explanation for our observations. However, this regulation is a property only of the longer isoform of activase produced by alternate splicing in some species. Tobacco lacks this isoform and does not show this kind of regulation in vitro (Zhang and Portis, 1999). Nevertheless, our data indicate that the activity of activase in tobacco may also be regulated by the thioredoxin system by an as-yet-unknown mechanism.

Role of RuBP

RuBP modulates Rubisco activity in vivo. It binds tightly to uncarbamyated active sites, blocking the carbamylation process, and removing RuBP from these sites is a primary function of activase. On the other hand, it has also been suggested that Rubisco carbamylation is directly modulated by RuBP (Mate et al., 1996). There are observations showing that a low steady-state RuBP concentration may cause Rubisco to decarbamylate, such that the rate of RuBP consumption is matched with its regeneration rate (Mott et al., 1984; Sage, 1990). In our study, as well as the previous one (Price et al., 1995a), Rubisco carbamylation remained high in anti-GAPDH plants despite low RuBP concentrations. Even at 700 μbar CO_2 , when the RuBP pools in anti-GAPDH plants decreased below the Rubisco site concentration (Table I), the Rubisco carbamylation state remained high (Table II).

A recent in vitro study demonstrated that subsaturating CO_2 combined with subsaturating RuBP causes Rubisco to decarbamylate, but Rubisco activase can prevent this decarbamylation (Portis et al., 1995). It is therefore possible that the maintenance of the high Rubisco carbamylation state in the anti-GAPDH plants was due to a high activity of Rubisco activase counteracting the tendency of Rubisco to decarbamylate when RuBP is scarce. This is supported by the high concentration of ATP, the elevated ATP/ADP ratio (Table II), and the high ΔpH (Price et al., 1995a), all of which are thought to promote the functioning of Rubisco activase (Portis, 1992). Alternatively, the high carbamylation state maintained in anti-GAPDH plants may also indicate that, in the absence of RuBP, binding of other chloroplast metabolites such as 3-PGA to Rubisco sites can prevent decarbamylation (Badger and Lorimer, 1981).

In some cases the manipulation of chloroplast metabolism has actually increased the activation of Rubisco. Elevated Rubisco activation levels (measured as the ratio between initial and total activities) have been observed in tobacco plants with reduced amounts of Rubisco (Quick et al., 1991) and phosphoribulokinase (Paul et al., 1996). However, those measurements were made at lower irradiances. The anti-phosphoribulosekinase plants are comparable to the anti-GAPDH plants, since both have high ATP/ADP

ratios and reduced RuBP contents. The activation state of Rubisco in anti-GAPDH plants was not higher than in control plants, whether measured as carbamylation state (Fig. 4B) or as a ratio between initial and total activity of Rubisco (data not shown). This can probably be explained by the high light intensity used in our measurements. It may be that the 80% carbamylation state routinely measured in tobacco leaves at high light is the upper limit for carbamylation.

In Vitro Activity

Phosphorylated sugars can bind tightly either to uncarbamylation sites, preventing activation, or to carbamylation sites, inhibiting catalysis. In vivo, Rubisco activase facilitates the dissociation of these compounds from active sites. The presence of tightly binding inhibitors in Rubisco sites can be detected as a decrease in the catalytic rate measured under substrate saturation (Seemann et al., 1985; Keys et al., 1995; Parry et al., 1997). We measured the carbamylated and total Rubisco site concentrations, as well as initial and total activities, and calculated the catalytic turnover rates of Rubisco sites. The turnover rates of the carbamylated sites in both anti-*bff* and anti-GAPDH plants were comparable to control values (Fig. 4, C and D), indicating that the carbamylated sites were free from inhibitory ligands after extraction. However, the total activity per total sites in the anti-*bff* plants declined as the Cyt *bff* content decreased (Fig. 4E). The reason for this could be that the uncarbamylation sites had tightly bound inhibitory compounds, which did not dissociate during the 5-min activating incubation. Nevertheless, during the carbamylation assays these inhibitory ligands were displaced by [¹⁴C]CPBP, which has very high affinity to Rubisco sites.

It is possible that the presence of inhibitors in Rubisco sites in anti-*bff* plants is another consequence of the decreased activity of Rubisco activase, in addition to the lowered carbamylation state. Studies with anti-activase tobacco plants discovered a slight impairment in the in vitro turnover rates of both carbamylated and uncarbamylation Rubisco sites (He et al., 1997). A tight-binding inhibitor of Rubisco has recently been found in tobacco leaves in the light (Parry et al., 1997). However, endogenous inhibitors are not the only factors that can decrease Rubisco activities measured in vitro. Rubisco extracted from leaves may be partially degraded by endogenous proteases (Servaites, 1985) or may be inhibited by polyphenolics (Bahr et al., 1981) and polyphenol oxidase (Koivuniemi et al., 1980), all of which are abundant in tobacco leaves. It is therefore possible that the decrease in the total catalytic activity of Rubisco in anti-*bff* plants is the result of direct inactivation. The difference in catalytic turnover rates between greenhouse-grown and growth-cabinet-grown wild-type plants may be attributable to the same phenomena (Table III).

In Vivo Catalysis

Studies of transgenic tobacco plants with severely reduced amounts of Rubisco activase show that not only carbamylation, but also in vivo turnover rates of carbamy-

lated Rubisco sites, are impaired by the lack of activase (He et al., 1997). As both RuBP content and RuBP/3-PGA ratios are high in anti-activase plants, the low Rubisco turnover rate can be deduced as resulting from the lack of activase. Since the RuBP concentrations and the RuBP/3-PGA ratio are lowered in both anti-GAPDH and anti-*bff* plants, we cannot judge if there is any additional decrease in the catalysis of Rubisco in the anti-*bff* plants, other than that which would be expected from the substrate limitation by RuBP (Fig. 5).

ACKNOWLEDGMENTS

We thank Prof. Ross McC. Lilley from the University of Wollongong for the advice with the luminometric assays, Dr. D. Büssis for advice on the GAPDH assays, and Dr. J.R. Evans for helpful discussions.

Received July 2, 1999; accepted October 12, 1999.

LITERATURE CITED

- Anderson JM, Price DG, Chow WS, Hope AB, Badger MR (1997) Reduced levels of cytochrome *bff* complex in transgenic tobacco leads to marked photochemical reduction of the plastoquinone pool, without significant change in acclimation to irradiance. *Photosynth Res* 53: 215–227
- Andrews TJ, Lorimer GH (1987) Rubisco: Structure, mechanisms, and prospects for improvement. In MD Hatch, NK Boardman, eds, *The Biochemistry of Plants: A Comprehensive Treatise*, Vol 10: Photosynthesis. Academic Press, New York, pp 131–218
- Badger MR, Lorimer GH (1981) Interaction of sugar phosphates with the catalytic site of ribulose-1,5-bisphosphate carboxylase. *Biochemistry* 20: 2219–2225
- Badger MR, Sharkey TD, von Caemmerer S (1984) The relationship between steady-state gas exchange of bean leaves and the levels of carbon-reduction cycle intermediates. *Planta* 160: 305–313
- Bahr JT, Johal S, Capel M, Bourque D (1981) High specific activity ribulose 1,5-bisphosphate carboxylase oxygenase from *Nicotiana tabacum*. *Photosynth Res* 2: 235–242
- Barkan A, Miles D, Taylor WC (1986) Chloroplast gene expression in nuclear photosynthetic mutants of maize. *EMBO J* 5: 1421–1427
- Bergmeyer J, Grassl M (1985) Tri- and dicarboxylic acid, purines, pyrimidines and derivatives, coenzymes, inorganic compounds. In H-U Bergmeyer, ed, *Methods of Enzymatic Analysis*, Vol VII: Metabolites 2. VCH Verlagsgesellschaft, Weinheim, Germany
- Biotto PA, Siegenthaler PA (1994) Variations of adenyly nucleotide content in two potato cultivars stored at 15°C: I. Method for the determination of ATP levels and first results. *Potato Res* 37: 151–160
- Brooks A, Portis AR Jr, Sharkey TD (1988a) Effects of irradiance and methyl viologen treatment on ATP, ADP, and activation of ribulose bisphosphate carboxylase in spinach leaves. *Plant Physiol* 88: 850–853
- Brooks A, Woo KC, Wong SC (1988b) Effects of phosphorus nutrition on the response of photosynthesis to CO₂ and O₂, activation of ribulose bisphosphate carboxylase and amounts of ribulose bisphosphate and 3-phosphoglycerate in spinach leaves. *Photosynth Res* 15: 133–141
- Buchanan BB (1984) The ferredoxin/thioredoxin system: a key element in the regulatory function of light in photosynthesis. *Bioscience* 34: 378–383
- Butz ND, Sharkey TD (1989) Activity ratios of ribulose-1,5-bisphosphate carboxylase accurately reflect carbamylation ratios. *Plant Physiol* 89: 735–739
- Campbell WJ, Ögren WL (1990a) Electron transport through photosystem I stimulates light activation of ribulose bisphosphate carboxylase/oxygenase (Rubisco) by Rubisco activase. *Plant Physiol* 94: 479–484

- Campbell WJ, Ogren WL** (1990b) A novel role for light in the activation of ribulosebiphosphate carboxylase/oxygenase. *Plant Physiol* **92**: 110–115
- Campbell WJ, Ogren WL** (1992) Light activation of Rubisco by Rubisco activase and thylakoid membranes. *Plant Cell Physiol* **33**: 751–756
- Dietz KJ, Heber U** (1984) Rate-limiting factors in leaf photosynthesis. I. Carbon fluxes in the Calvin cycle. *Biochim Biophys Acta* **767**: 432–443
- Farquhar GD, von Caemmerer S, Berry JA** (1980) A biochemical model of photosynthetic CO₂ assimilation in leaves of C₃ species. *Planta* **149**: 78–90
- Foyer C** (1993) Interactions between electron transport and carbon assimilation in leaves: coordination of activities and control. *In* YP Abrol, P Mohanty, Govindjee, eds, *Photosynthesis: Photoreactions to Plant Productivity*. Kluwer Academic Publishers, Dordrecht, The Netherlands, pp 199–224
- Gardeström P** (1987) Adenylate ratios in the cytosol, chloroplasts and mitochondria of barley leaf protoplasts during photosynthesis at different carbon dioxide concentrations. *FEBS Lett* **212**: 114–118
- Gardeström P, Wigge B** (1988) Influence of photorespiration on ATP/ADP ratios in the chloroplasts, mitochondria, and cytosol, studied by rapid fractionation of barley (*Hordeum vulgare*) protoplasts. *Plant Physiol* **88**: 96–76
- Gilmore AM, Björkman O** (1994) Adenine nucleotides and the xanthophyll cycle in leaves: I. Effects of CO₂- and temperature-limited photosynthesis on adenylate energy charge and violaxanthin de-epoxidation. *Planta* **192**: 526–536
- Grace SC, Logan BA** (1996) Acclimation of foliar antioxidant systems to growth irradiance in three broad-leaf evergreen species. *Plant Physiol* **112**: 1631–1640
- Grana X, Urena J, Ludevid D, Carreras J, Climent F** (1989) Purification, characterization and immunological properties of 2,3-bisphosphoglycerate-independent phosphoglycerate mutase from maize (*Zea mays*) seeds. *Eur J Biochem* **186**: 149–153
- Grisolia S, Carreras J** (1975) Phosphoglycerate mutase from wheat germ (2,3-PGA independent). *Methods Enzymol* **42**: 429–435
- Harbinson J, Genty B, Foyer C** (1990) Relationship between photosynthetic electron transport and stromal enzyme activity in pea leaves. *Plant Physiol* **94**: 545–553
- Hauser M, Eichelmann H, Heber U, Laisk A** (1995a) Chloroplast pH values and buffer capacities in darkened leaves as revealed by CO₂ solubilization in vivo. *Planta* **196**: 199–204
- Hauser M, Eichelmann H, Oja V, Heber U, Laisk A** (1995b) Stimulation by light of rapid pH regulation in the chloroplast stroma in vivo as indicated by CO₂ solubilization in leaves. *Plant Physiol* **108**: 1059–1066
- He Z, von Caemmerer S, Hudson GS, Price GD, Badger MR, Andrews TJ** (1997) Ribulose-1,5-bisphosphate carboxylase/oxygenase activase deficiency delays senescence of ribulose-1,5-bisphosphate carboxylase/oxygenase but progressively impairs its catalysis during tobacco leaf development. *Plant Physiol* **115**: 1569–1580
- Heineke D, Riens B, Grosse H, Hoferichter P, Peter U, Flüge U-I, Heldt HW** (1991) Redox transfer across the inner envelope membrane. *Plant Physiol* **95**: 1131–1137
- Heldt HW** (1979) Light-dependent changes of stromal H⁺ and Mg⁺² concentration controlling CO₂ fixation. *In* M Gibbs, E Latzko, eds, *Encyclopedia of Plant Physiology*, Vol 6: Photosynthesis II. Springer-Verlag, Berlin, pp 202–207
- Hewitt EJ, Smith TA** (1975) *Plant Mineral Nutrition*. English University Press, London
- Holfgrefe S, Backhausen JE, Kitzmann C, Scheibe R** (1997) Regulation of steady-state photosynthesis in isolated intact chloroplasts under constant light: responses of carbon fluxes, metabolite pools and enzyme-activation states to changes of electron pressure. *Plant Cell Physiol* **38**: 1207–1216
- Ikuma H, Tetley RM** (1976) Possible interference by an acid-stable enzyme during the extraction of nucleoside di- and triphosphates from higher plant tissues. *Plant Physiol* **58**: 320–323
- Keys AJ, Major I, Parry MAJ** (1995) Is there another player in the game of Rubisco regulation? *J Exp Bot* **46**: 1245–1251
- Koivuniemi PJ, Tolbert NE, Carlson PS** (1980) Ribulose-1,5-bisphosphate carboxylase-oxygenase and polyphenol oxidase in the tobacco mutant su-su and 3 green revertant plants. *Plant Physiol* **65**: 828–833
- Krall JP, Sheveleva EV, Pearcy RW** (1995) Regulation of photosynthetic induction state in high- and low-light-grown soybean and *Alocasia macrorrhiza* (L.) G. Don. *Plant Physiol* **109**: 307–317
- Lauerer M, Saffic D, Quick WP, Labate C, Fichtner K, Schulze E-D, Rodermeil SR, Bogorad L, Stitt M** (1993) Decreased ribulose-1,5-bisphosphate carboxylase-oxygenase in transgenic tobacco transformed with 'antisense' *rbcS*. VI. Effect on photosynthesis in plants grown at different irradiance. *Planta* **190**: 332–345
- Leadlay PF, Breatnach R, Gatehouse JA, Johnson PE, Knowles JR** (1977) Phosphoglycerate mutase from wheat germ: isolation, crystallisation and properties. *Biochemistry* **16**: 3050–3053
- Lilley RM, Grahame PG, Ali SRM** (1985) Determination of picomole amounts of glycerate 3-phosphate, glycerate 2-phosphate and phosphoenolpyruvate by an enzymic assay coupled to firefly luciferase/luciferin luminescence. *Anal Biochem* **148**: 282–287
- Lorimer GH, Badger MR, Andrews TJ** (1976) The activation of ribulose-1,5-bisphosphate carboxylase by carbon dioxide and magnesium ions: equilibria, kinetics, a suggested mechanism and physiological implications. *Biochemistry* **15**: 529–536
- Mächler F, Nösberger T** (1980) Regulation of ribulose biphosphate carboxylase activity in intact wheat leaves by light, CO₂ and temperature. *J Exp Bot* **35**: 1485–1491
- Mate CJ, Hudson GS, von Caemmerer S, Evans JR, Andrews TJ** (1993) Reduction of ribulose biphosphate carboxylase activase levels in tobacco (*Nicotiana tabacum*) by antisense RNA reduces ribulose bisphosphate carboxylase carbamylation and impairs photosynthesis. *Plant Physiol* **102**: 1119–1128
- Mate CJ, von Caemmerer S, Evans JR, Hudson GS, Andrews TJ** (1996) The relationship between CO₂-assimilation rate, Rubisco carbamylation and Rubisco activase content in activase-deficient transgenic tobacco suggests a simple model of activase action. *Planta* **198**: 604–613
- Mott KA, Jensen RG, O'Leary JW, Berry JA** (1984) Photosynthesis and ribulose 1,5-bisphosphate concentrations in intact leaves of *Xanthium strumarium* L. *Plant Physiol* **76**: 968–971
- Parry MAJ, Andralojc PJ, Parmar S, Keys AJ, Habash D, Paul MJ, Alred R, Quick WP, Servaites JC** (1997) Regulation of Rubisco by inhibitors in the light. *Plant Cell Environ* **20**: 528–534
- Paul MJ, Andralojc PJ, Banks FM, Parry MAJ, Knight JS, Gray JC, Keys AJ** (1996) Altered Rubisco activity and amounts of a daytime tight-binding inhibitor in transgenic tobacco expressing limiting amounts of phosphoribulokinase. *J Exp Bot* **47**: 1963–1966
- Portis AR Jr** (1981) Evidence of a low stromal Mg²⁺ concentration in intact chloroplasts in the dark. 1. Studies with the ionophore A23187. *Plant Physiol* **67**: 985–989
- Portis AR Jr** (1992) Regulation of ribulose-1,5-bisphosphate carboxylase/oxygenase activity. *Annu Rev Plant Physiol Plant Mol Biol* **43**: 415–437
- Portis AR Jr** (1995) The regulation of Rubisco by Rubisco activase. *J Exp Bot* **46**: 1285–1291
- Portis AR Jr, Lilley RM, Andrews TJ** (1995) Subsaturating ribulose-1,5-bisphosphate concentration promotes inactivation of ribulose-1,5-bisphosphate carboxylase/oxygenase (Rubisco): studies using continuous substrate addition in the presence and absence of Rubisco activase. *Plant Physiol* **109**: 1441–1451
- Price GD, Evans JR, von Caemmerer S, Yu J-W, Badger MR** (1995a) Specific reduction of chloroplast glyceraldehyde-3-phosphate dehydrogenase activity by antisense RNA reduces CO₂ assimilation via a reduction in ribulose bisphosphate regeneration in transgenic tobacco plants. *Planta* **195**: 369–378
- Price GD, von Caemmerer S, Evans JR, Siebke K, Anderson JM, Badger MR** (1998) Photosynthesis is strongly reduced by antisense suppression of chloroplast cytochrome *b/f* complex in transgenic tobacco. *Aust J Plant Physiol* **25**: 445–452
- Price GD, Yu J-W, von Caemmerer S, Evans JR, Chow WS, Anderson JM, Hurry V, Badger MR** (1995b) Chloroplast cyto-

- chrome *b₆/f* and ATP synthase complexes in tobacco: transformation with antisense RNA against nuclear-encoded transcripts for the Rieske FeS and ATP δ polypeptides. *Aust J Plant Physiol* **22**: 285–297
- Quick WP, Schurr U, Scheibe R, Schulze E-D, Rodermel SR, Bogorad L, Stitt M (1991) Decreased ribulose-1,5-bisphosphate carboxylase-oxygenase in transgenic tobacco transformed with “antisense” *rbcS*. I. Impact on photosynthesis in ambient growth conditions. *Planta* **183**: 542–554
- Robinson SP, Portis AR Jr (1988) Involvement of stromal ATP in the light activation of ribulose-1,5-bisphosphate carboxylase-oxygenase in intact isolated chloroplasts. *Plant Physiol* **86**: 293–298
- Ruuska SA (1998) Interactions between photosynthetic electron transport and carbon assimilation in transgenic tobaccos impaired in photosynthesis. PhD thesis. Australian National University, Canberra
- Ruuska SA, Andrews TJ, Badger MR, Hudson GS, Laisk A, Price GD, von Caemmerer S (1998) The interplay between limiting processes in C_3 photosynthesis studied by rapid-response gas exchange using transgenic tobacco impaired in photosynthesis. *Aust J Plant Physiol* **25**: 859–870
- Sage RF (1990) A model describing the regulation of ribulose-1,5-bisphosphate carboxylase, electron transport, and triose phosphate use in response to light intensity and CO_2 in C_3 plants. *Plant Physiol* **94**: 1728–1734
- Sage RF, Sharkey TD, Seemann J (1990) Regulation of ribulose-1,5-bisphosphate carboxylase oxygenase activity in response to light intensity and CO_2 in the C_3 annuals *Chenopodium album* L. and *Phaseolus vulgaris* L. *Plant Physiol* **94**: 1735–1742
- Salvucci ME, Portis AR Jr, Ogren WL (1985) A soluble chloroplast protein catalyzes ribulosebisphosphate carboxylase oxygenase activation in vivo (technical note). *Photosynth Res* **7**: 193–201
- Scheibe R (1987) NADP⁺ malate dehydrogenase in C_3 plants: regulation and role of a light-activated enzyme. *Physiol Plant* **71**: 393–400
- Scheibe R, Jacquot J-P (1983) NADP regulates the light activation of NADP-dependent malate dehydrogenase. *Planta* **157**: 548–553
- Scheibe R, Stitt M (1988) Comparison of NADP-malate dehydrogenase activation, Q_A reduction and O_2 reduction in spinach leaves. *Plant Physiol Biochem* **26**: 473–481
- Seemann JR, Berry JA, Freas S, Krump MA (1985) Regulation of ribulose bisphosphate carboxylase activity *in vivo* by a light-modulated inhibitor of catalysis. *Proc Natl Acad Sci USA* **82**: 8024–8028
- Seemann JR, Sharkey TD, Wang J, Osmond CB (1987) Environmental effects on photosynthesis, nitrogen-use efficiency and metabolite pools in leaves of sun and shade plants. *Plant Physiol* **84**: 796–802
- Servaites JC (1985) Crystalline ribulose bisphosphate carboxylase/oxygenase of high integrity and catalytic activity from *Nicotiana tabacum*. *Arch Biochem Biophys* **238**: 154–160
- Sharkey TD (1990) Feedback limitation of photosynthesis and the physiological role of ribulose bisphosphate carboxylase carbamylation. *Bot Mag Tokyo* **2**: 87–105
- Smith GS, Hass LF (1985) Wheat germ phosphoglycerate mutase: purification, polymorphism and inhibition. *Biochem Biophys Res Commun* **131**: 743–749
- Somerville SC, Portis AR Jr, Ogren WL (1982) A mutant of *Arabidopsis thaliana* which lacks activation of RuBP carboxylase *in vivo*. *Plant Physiol* **70**: 381–387
- Stitt M (1996) Metabolic regulation of photosynthesis. *Adv Photosynth* **5**: 151–190
- Stitt M, Lilley RM, Gerhardt R, Heldt HW (1989) Metabolite levels in specific cells and subcellular compartments of plant leaves. *Methods Enzymol* **174**: 518–552
- Stitt M, Lilley RM, Heldt HW (1982) Adenine nucleotide levels in the cytosol, chloroplasts, and mitochondria of wheat leaf protoplasts. *Plant Physiol* **70**: 971–977
- von Caemmerer S, Edmondson DL (1986) Relationship between steady-state gas-exchange, *in vivo* ribulose bisphosphate carboxylase activity and some carbon-reduction cycle intermediates in *Raphanus sativus*. *Aust J Plant Physiol* **13**: 669–688
- von Caemmerer S, Farquhar GD (1981) Some relationships between the biochemistry of photosynthesis and the gas exchange of leaves. *Planta* **153**: 376–387
- Wang ZY, Portis AR Jr (1992) Dissociation of ribulose-1,5-bisphosphate bound to ribulose-1,5-bisphosphate carboxylase/oxygenase and its enhancement by ribulose-1,5-bisphosphate carboxylase/oxygenase activase-mediated hydrolysis of ATP. *Plant Physiol* **99**: 1348–1353
- Wulff K, Doppen W (1985) ATP: luminometric method. In H-U Bergmeyer, ed, *Methods of Enzymatic Analysis*, Vol VII. VCH Verlagsgesellschaft, Basel, pp 357–364
- Zhang N, Portis AR Jr (1999) Mechanism of light regulation of Rubisco: a specific role for the larger Rubisco activase isoform involving reductive activation by thioredoxin-f. *Proc Natl Acad Sci USA* **96**: 9438–9443